ELSEVIER

International Journal of Pharmaceutics 244 (2002) 169–179

international journal of pharmaceutics

www.elsevier.com/locate/ijpharm

Kinetics of the radicals induced in gamma-irradiated naproxen sodium and apranax
Applicability of ESR technique to monitor radiosterilization of naproxen sodium-containing drugs

M. Polat *, M. Korkmaz

Physics Engineering Department, Hacettepe University, Beytepe, Ankara, Turkey

Received 18 February 2002; received in revised form 14 June 2002; accepted 21 June 2002

Abstract

In the present work the spectroscopic and kinetic features of the radicals induced in gamma-irradiated naproxen sodium (NS) and apranax (AP) tablet are investigated at room and different temperatures in the dose range of 2.5–25 kGy by electron spin resonance technique (ESR). Radiation produces two different radicals (I, II) in NS quite stable at room temperature but relatively unstable above room temperature, giving rise to a broad singlet centered at $g = 2.0057$. Dose–response and decay curves associated with the broad singlet were found to follow bi-exponentials. Information concerning the saturation decay rates and activation energies were obtained through the characteristics of these exponentials. Similar calculations were also performed for AP, which contains 550 mg NS as active ingredient, and the applicability of ESR technique for monitoring radiosterilization of AP was discussed.

Keywords: ESR; Naproxen sodium; Radiation; Sterilization

1. Introduction

Ethylene oxide and autoclave techniques are frequently used to sterilize drugs, drug raw materials and medical supplies. However, ethylene oxide residue and decomposition at high temperatures create difficulties in sterilizing drugs and drug raw materials by these techniques. Sterilization by radiation is used to overcome these difficulties (Christensen et al., 1967; Gaughran and Goudie, 1977; Safrany, 1997; Pourahmad and Pakravan, 1997; Jacobs, 1991; Reid, 1995; Duroux et al., 1996). Nevertheless, besides its advantages such as high penetrability, homogeneous sterilization and sterilizability of final package form, radiosterilization also has some drawbacks. Radiosensitivity of the irradiated pharmaceutical is especially important in radiosterilization because radiation can cause a decrease in the amount of active drug ingredient by destroying it and,

* Corresponding author. Tel.: +90-312-297-72-13; fax: +90-312-299-20-37

E-mail address: polat@hacettepe.edu.tr (M. Polat).

0378-5173/02/$ - see front matter
PII: S0378-5173(02)00329-0

therefore, creating reactive molecular fragments (Schuler, 1994; Boess and Bögl, 1996; Gibella et al., 2000; Jacobs, 1995; Miyazaki et al., 1994) which may result in a toxicological hazard. The species and amount of the molecular fragments or radicals possessing unpaired electron created by radiation can be best detected by electron spin resonance (ESR) spectroscopy which is frequently used to measure the absorbed dose of an irradiated material (Dood et al., 1985; Basly et al., 1998; Polat et al., 1997; Korkmaz and Polat, 2000, 2001; Onori et al., 1996; Desrosiers and Simie, 1988; Raffi, 1992; Bögl, 1989).

Naproxen or naproxen sodium (NS)-based products accounts for nearly one in every five prescriptions written for nonsteroidal anti-inflammatory drugs (NSAIDs). Naproxen has been used safely and effectively worldwide for more than 20 years, and is one of the most widely used drugs to treat mild-to-moderate pain, osteoarthritis, rheumatoid arthritis, ankylosing spondylitis, primary dysmenorrhea, tendinitis, bursitis, and other conditions. Naproxen or NS-based drugs such as apranax fort and apranax (AP) are mainly administered orally. However, their administration by dispersing these nonsteroidal anti-inflammatory drugs into biodegradable polymer matrices has also been accepted as a good approach for obtaining a therapeutic effect in a predetermined period of time, meanwhile minimizing side effects (Bozdağ et al., 2001; Çaliş et al., 2002). Nevertheless, the parenteral drug delivery systems created by this approach have to meet the pharmacopoeial requirements of sterility. The chemical liability of naproxen and NS and polymeric matrix materials generally limits the strategies for obtaining an acceptable sterile product to aseptic processing. Terminal sterilization by gamma irradiation of the parenteral drug delivery systems would be preferred from a microbiological safety point of view, since aseptic processing is inherently more risky with respect to microbial contamination of the finished product (Çaliş et al., 2002; Volland et al., 1994). Since polymer-based drug delivery systems are very sensitive to dry or moist heat, and ethylene oxide is not applicable due to its toxic residues, gamma irradiation currently remains the only accepted method for terminal sterilization of these systems. However, radiolytic degradation of incorporated drug and polymer matrix might be considered as the principle potential disadvantage of terminal gamma sterilization (Bittner et al., 1999).

There does not exist any data relative to the radiosensitivities of naproxen or NS in the literature. Therefore, the aim of the present work is twofold: first, investigate the radiation sensitivity of NS and AP in the dose range of 2.5–25 kGy, and second, explore the possibility of using ESR technique to monitor the radiosterilization of AP and parenteral drug delivery system containing NS as the active ingredient, through a kinetic study of the radiation-induced radicals by ESR spectroscopy.

2. Materials and methods

NS, its chemical name is 2-naphthaleneacetic acid, 6-methoxy-α-methyl sodium salt ($C_{14}H_{13}NaO_3$), and AP 550 mg tablets were provided from Abdi Ibrahim Drug Company (Istanbul, Turkey). NS is an odourless, crystalline powder white-to-creamy in color and has a molecular structure as given in Fig. 1. It is soluble in methanol and water. As for AP tablets, they are coated with a blue coating suspension, and each AP tablet is known to contain NS as an active ingredient, with lactose, magnesium stearate, and microcrystalline cellulose as excipients. The coating suspension is supposed to contain hydroxyprophyl methyl cellulose, opaspray, polyethylene glycol or opadry. Coating films of four AP tablets were skinned carefully from the rest, and they are irradiated separately in order to avoid any possible

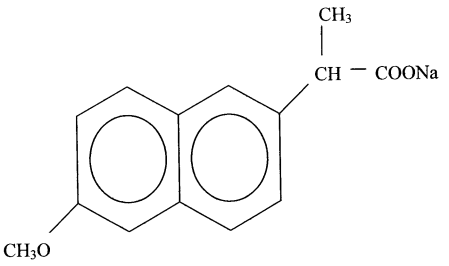

Fig. 1. Molecular structure of NS.

contribution(s) complicating the ESR spectra. After skinning the tablets from their coating films they are ground mechanically and irradiated, while NS is irradiated as it was received. All irradiations were performed at room temperature (290 K) using a ^{60}Co gamma cell supplying a dose rate of 2.5 kGy/h as an ionizing radiation source at the Sarayköy Establishment of Turkish Atomic Energy Agency in Ankara. The dose rate at the sample sites was measured by s Fricke dosimeter.

ESR measurements were carried out using a Varian 9" E-L X-band ESR spectrometer operating at 9.5 GHz and equipped with a TE_{104} rectangular double cavity containing a DPPH standard sample in the rear resonator which remained untouched throughout all the experiment. The spectrometer operating conditions adopted during the experiment are given in Table 1. The spectra were recorded at room and different temperatures. Signal intensities were calculated from the first derivative spectra and compared with the spectra obtained for a standard DPPH sample under the same spectrometer operating conditions. Sample temperature inside the microwave cavity was monitored with a digital temperature control system (Bruker ER 4111-VT). The latter provided the opportunity of measuring the temperature with an accuracy of ± 0.5 K at the site of the sample. A cooling, heating and subsequent cooling cycle was adopted to monitor free radical signal evaluations. The temperature of the samples was first decreased to 125 K, starting from room temperature with an increment of 20 K, then increased to 400 K and finally decreased again to room temperature.

Kinetic studies of the free radicals were performed at different temperatures. To achieve this goal, the samples were heated to a predetermined temperature and kept at this temperature for a predetermined time, then they were cooled to room temperature and their spectra were recorded. Adopted predetermined temperatures and times were 308, 323, 338, 358, 373 K and 3, 6, 10, 15, 25, 40, 60, 90 min in the present study. The results were the average of five replicates for each radiation dose.

Table 1
ESR spectrometer operating conditions adopted throughout the experiment

Central field	329 mT
Sweep width	20 mT
Microwave frequency	9.26 GHz
Microwave power	1 mW
Modulation frequency	100 kHz
Modulation amplitude	0.5 mT
Receiver gain	5×10^3–5×10^2
Scan time	240 s
Time constant	1 s
Temperature	125–400 K

3. Experimental results and discussion

3.1. NS

Although unirradiated NS exhibited no ESR signal, irradiated NS showed a very simple ESR spectrum consisting of a broadened antisymmetric single resonance line as shown in Fig. 2a. Variation of the peak-to-peak height of this resonance line with applied microwave power indicated that we are dealing with a homogeneously broadened line (Fig. 3a) arising from more than one radical species whose g-values depend on the orientation of external magnetic field with respect to the molecular axes. As for variation of the peak-to-

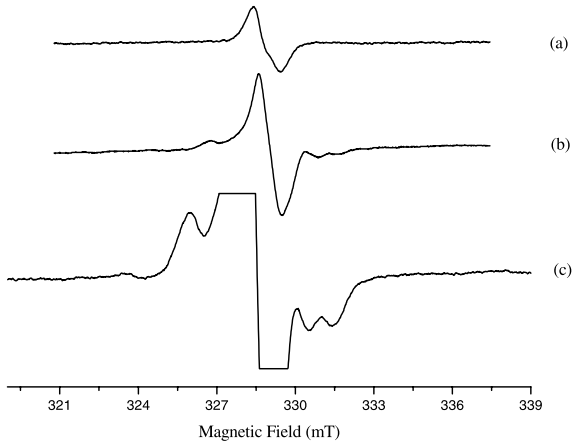

Fig. 2. ESR spectra of irradiated NS and AP tablet—(a) NS irradiated at 15 kGy, (b) AP irradiated at 15 kGy, (c) same as b but modulation amplitude is 1 mT.

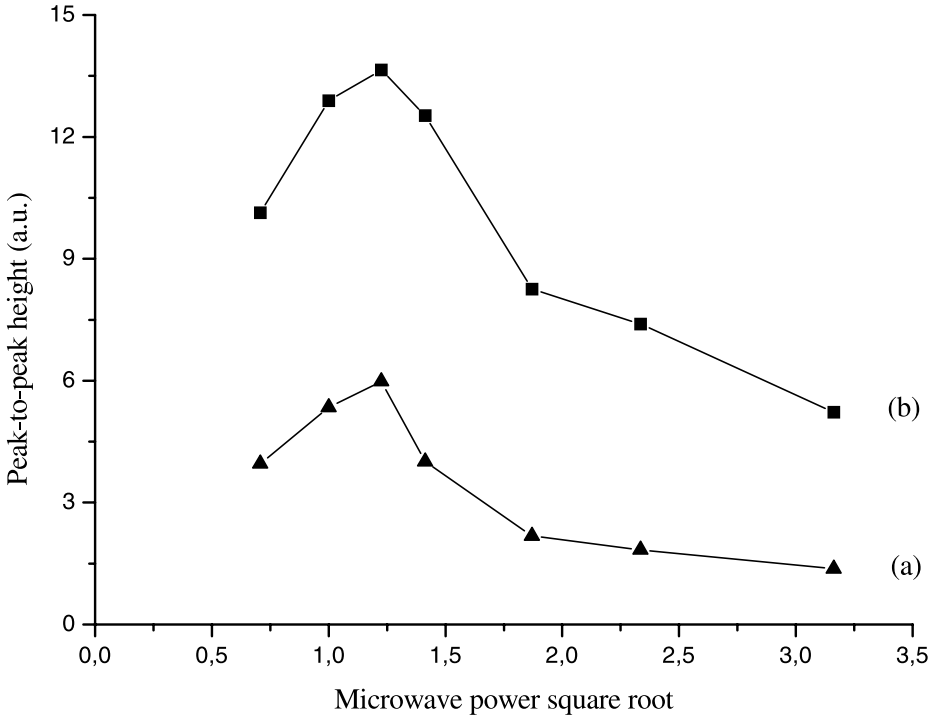

Fig. 3. Variation of ESR peak-to-peak heights with applied microwave power—(a) NS, (b) AP.

peak height of this resonance line with absorbed dose, it was found that it follows the sum of two exponential curves of the type $I = 22.7 \times (1 - e^{-D/33.4})$ and $II = 44.5 \times (1 - e^{-D/24.4})$ in dose range of 2.5–25 kGy (Fig. 4a). In the last expressions D stands for the absorbed dose in kGy. It is seen from Fig. 4a that two radicals of different saturation character contribute to the dose–response curve of NS which starts to saturate around 20 kGy. The variation of ESR peak-to-peak height of irradiated NS with temperature was also investigated in the temperature range of 125–400 K. The results are given in Fig. 5a. The decrease in temperature produced practically no changes in the peak-to-peak height below room temperature. However, warming the sample above room temperature caused a decrease in the peak-to-peak height and this continued up to 400 K, which is the highest temperature reached in the present work. This decrease in peak-to-peak height was observed to be irreversible corresponding to an irreversible decay of responsible radicals.

The radical species responsible for ESR singlet observed for irradiated NS are expected to have different decay characteristics depending on the sample temperature. In other words, the decay rates of the radicals at high temperatures should be higher than the decay rates at low temperatures. In fact, it was found that it is the case. Radiation-induced radicals in NS were observed to be very stable at room temperature (Fig. 6a). However, an increase in temperature accelerated the decay of the radicals and the higher the temperature the higher the decay rates (Fig. 7) of the radicals. Experimental peak-to-peak height decay data obtained for samples kept at 308, 323, 338, 358 and 373 K were used to determine the decay rates at these temperatures by fitting the latter data to exponential functions, assuming that the contributing radical species follow second-order kinetics. Two radical species decaying with assumed kinetics were found to fit best the experimental results. Dashed lines in Fig. 7 show the theoretical curves obtained by this procedure. Relative

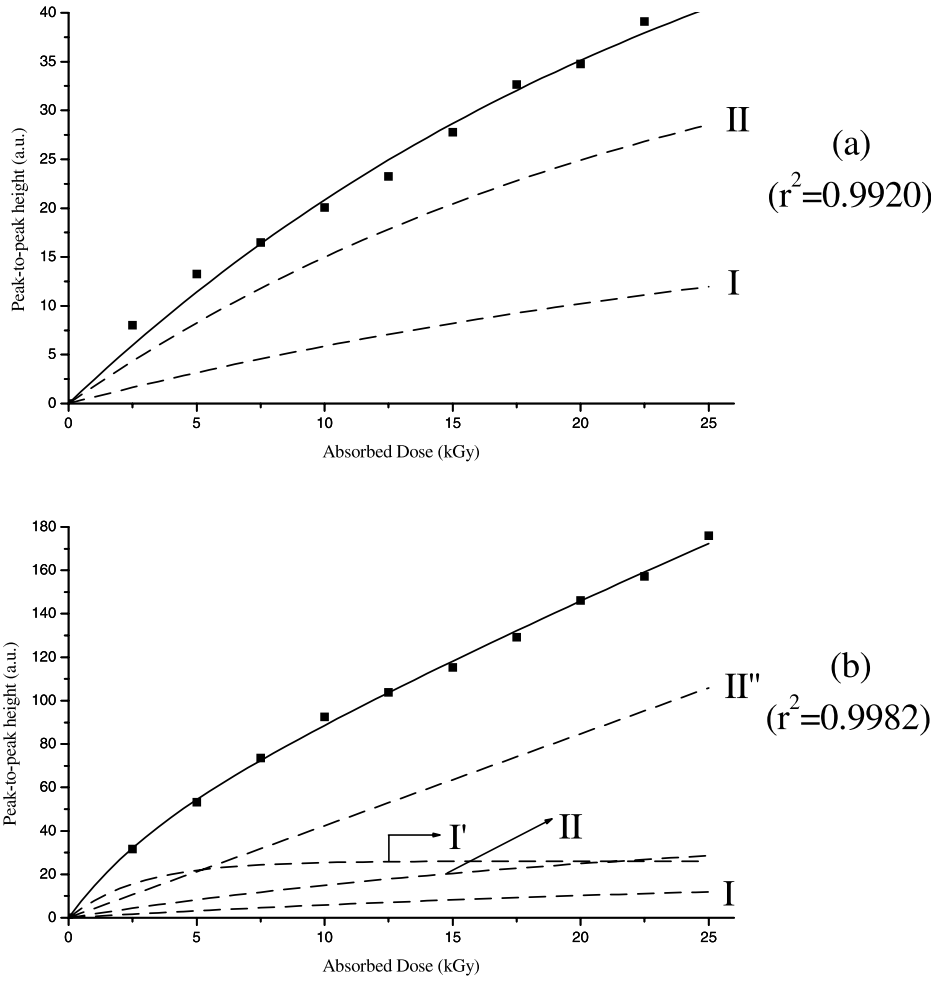

Fig. 4. Variation of ESR peak-to-peak heights with absorbed radiation dose(a) NS, (b) AP. Symbols, experimental; dashed and full lines, theoretical. Dashed lines were obtained by fitting experimental data to functions: $I = 22.7 \times (1 - e^{-D/33.4})$; $II = 44.5 \times (1 - e^{-D/24.4})$; $I' = 26.1 \times (1 - e^{-D/2.76})$; $II'' = 4.23 \times D$. Full lines are the sum of dashed lines.

weights and decay constants of the radicals contributing to the ESR singlet of the NS samples irradiated at a dose of 15 kGy are summarized in Table 2. An Arrhenius plot was also constructed to calculate the activation energies of the contributing radicals and the graph given in Fig. 8 was obtained.

3.2. AP

Unirradiated AP skinned from its coating film did not exhibit any resonance signal; however, irradiated AP did. A resonance line centered $g =$ 2.0057 dominates the ESR spectrum of AP, and two pairs of additional very weak lines appear at low- and high-field sides of this centerline when the spectra were recorded at high modulation amplitudes. Two spectra recorded for modulation amplitudes of 0.5 and 1 mT are given in Fig. 2b,c, respectively, for a sample irradiated at room temperature at 15 kGy. As is seen from Fig. 2b,c, centerline of irradiated AP has similar g-value with the singlet of the irradiated NS. This is an expected result due to countenance of AP. However, normalized peak-to-peak height of AP centerline is higher than that of NS. This results

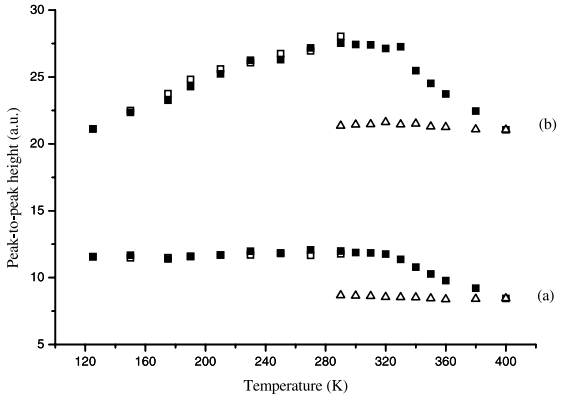

Fig. 5. Variation of ESR peak-to-peak heights with temperature—(a) NS, (b) AP. (□), cooling to liquid nitrogen temperature; (■), heating up to 400 K; and (△), cooling again to room temperature.

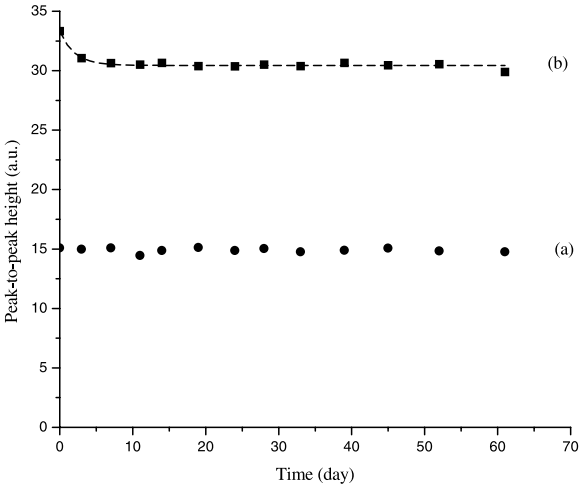

Fig. 6. Variation at room temperature of ESR peak-to-peak height with time elapsed after irradiation cessation—(a) NS, (b) AP.

from the presence of additional radiation-induced radical species having similar g-values with radicals I and II in the excipient part of AP tablet. Microwave saturation behavior of the radical species contributing to the centerline was similar to the behavior of radicals induced in pure NS (Fig. 3b). Peak-to-peak height of $g = 2.0057$ lines increases up to 1.5 mW and then starts to decrease, as in the case of irradiated NS. As for the variation of peak-to-peak height of the $g = 2.0057$ centerline

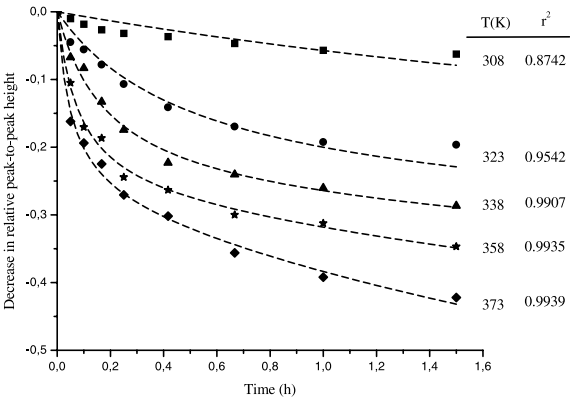

Fig. 7. Decrease in relative peak-to-peak height for NS samples irradiated at a dose of 15 kGy and kept at different temperatures. Symbols, experimental; dashed lines, sum of the calculated theoretical decays of two contributing radicals.

with absorbed dose, it increases with increase in dose. This increase in peak-to-peak height fits well with three exponential and one linear curves of the types $I = 22.7 \times (1 - e^{-D/33.4})$, $II = 44.5 \times (1 - e^{-D/24.4})$, $I' = 26.1 \times (1 - e^{-D/2.76})$ and $II'' = 4.23 \times D$, which indicate the contributions of two more radical species created in excipient part of AP to $g = 2.0057$ resonance line besides radicals arising directly from the presence of NS in AP (Fig. 4b). The variation of the peak-to-peak height of $g = 2.0057$ centerline of AP with temperature is a bit different than the variation of ESR peak-to-peak height observed for pure NS. Below room temperature the peak-to-peak height of $g = 2.0057$ centerline decreases with decrease in temperature; however, this decrease is reversible. Above room temperature, an irreversible decrease in peak-to-peak height is observed, as in the case of irradiated NS (Fig. 5a). Long-term decay of AP peak-to-peak height at room temperature with time elapsed after irradiation cessation is different than that observed for pure NS. At the beginning, signal decays relatively fast, but then the decay is very very slow (Fig. 6b). This indicates that the peak-to-peak height decay of AP at room temperature has a biphasic character.

Experimental results relative to the decay of peak-to-peak height of $g = 2.0057$ centerline at different temperatures are given in Fig. 9. As is expected, the higher the temperature the faster the decay. Comparison of the decay results of irra-

Table 2
Relative weights, decay constants and activation energies of the radicals contributing to the ESR signal of NS samples irradiated at a dose of 15 kGy

Radical	Temperature (K)	Relative weight	Decay constant (k)	Activation energy (kJ/mol)
I	308	0.286	1.4598	39.5±2.4
	323	0.286	2.2259	
	338	0.286	5.2925	
	358	0.286	12.0000	
	373	0.286	19.0506	
II	308	0.714	0.0054	51.4±1.2
	323	0.714	0.0145	
	338	0.714	0.0341	
	358	0.714	0.0839	
	373	0.714	0.1927	

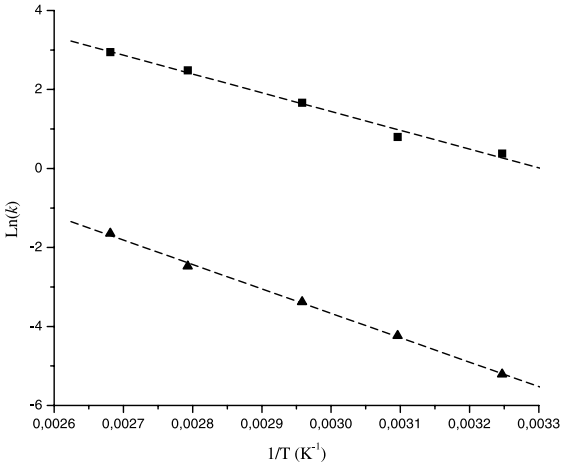

Fig. 8. Arrhenius plots constructed for irradiated NS. Upper line radical I, lower line radical II.

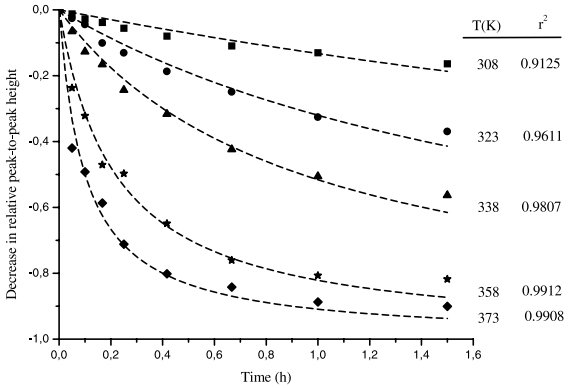

Fig. 9. Variation of ESR peak-to-peak height for AP samples irradiated at a dose of 15 kGy and kept at different temperatures. Symbols, experimental; dashed lines, sum of the theoretical decays of four contributing radicals.

diated NS with those of AP indicates that the decay of peak-to-peak height in AP is faster than the decay in pure NS. This proves once more the differences in the characteristics of the radical species produced in irradiated NS and AP. The decay constants and activation energies calculated assuming that the radical species contributing to the formation of centerline of AP follow second-order kinetics are given in Table 3. Dashed lines given in Fig. 9 are calculated using the decay constants of Table 3. Agreement between these lines and their corresponding experimental counterpart shows that the model basing on the second-order decays of four different radical species explains well the kinetic behavior of the contributing radicals at different annealing temperatures. An Arrhenius plot was also constructed to calculate the activation energies of the contributing radicals and the graph given in Fig. 10 was obtained.

Spectra simulation calculations were also performed, and parameters such as g-factor, line width and possible hyperfine splitting constants of the radiation-induced radicals contributing to the formations of the ESR spectra of NS and AP were also calculated. However, these data are not included in the present work.

Table 3
Relative weights, decay constants and activation energies of the radicals contributing to the ESR signal of AP samples irradiated at a dose of 15 kGy

Radical	Temperature (K)	Relative weight	Decay constant (per h)	Activation energy (kJ/mol)
I	308	0.082	0.3581	40.7 ± 1.1
	323	0.082	0.7395	
	338	0.082	1.3316	
	358	0.082	3.4058	
	373	0.082	5.5895	
II	308	0.1836	1.7941	53.7 ± 2.5
	323	0.1836	3.9271	
	338	0.1836	11.1529	
	358	0.1836	26.9262	
	373	0.1836	72.1827	
I′	308	0.0847	0.7000	31.8 ± 1.0
	323	0.0847	1.2118	
	338	0.0847	2.1999	
	358	0.0847	3.7162	
	373	0.0847	6.2808	
II″	308	0.6497	0.0350	81.1 ± 2.8
	323	0.6497	0.1402	
	338	0.6497	0.4818	
	358	0.6497	3.3868	
	373	0.6497	7.6561	

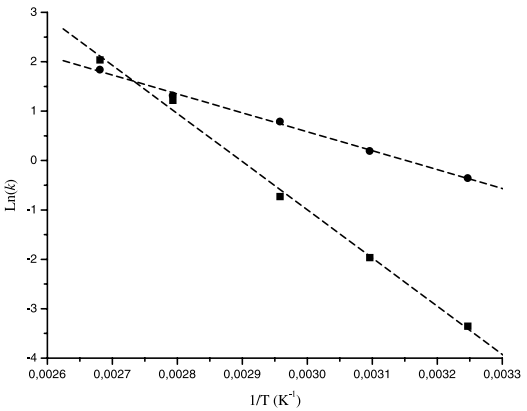

Fig. 10. Arrhenius plots constructed for irradiated AP. Upper line radical I′, lower line radical II″.

3.3. Mechanism of radical formations

Excited molecules are produced both directly and by neutralization of radical cations (Dusaucy and Tilquin, 1991). They may decompose to radicals by the rupture of chemical bonds. However, radicals which are molecular fragments do not diffuse in solid matrices due to cage effect, and immediate germinate termination reactions are possible (Tilquin, 1985). Excited molecules and radical cations are localized along the track in region of high local concentration. So the radicals are also formed in spurs and kinetic must take effect of non-homogeneous formation of the species into consideration.

The concentration of radicals in irradiated NS grows linearly at the beginning and then at a progressively lower rate, until a relatively steady plateau is reached in the dose range of 2.5–25 kGy. It appears that during irradiation radicals are removed by relatively rapid processes other than those which occur after the cessation of irradiation. Mechanisms that may contribute to the dose effect include the following:

– There exist physical and chemical scavengers for the trapping of the moving electrons. More and more radicals are trapped during radiolysis. These radicals present a better electron affinity

than the original molecule and therefore, are in competition to pick up electrons, which could be transferred, at long distance, through the tunneling effect.
– Part of the energy used to produce the initial radicals now favors the activation of solute radiolytic products. Therefore, the result is a deactivation of primary species producing the radical by energy transfer.

It is difficult to presume, a priori, the bond that would be ruptured by gamma irradiation, because NS contains many kinds of chemical bonds. However, independence of the signal shape from received dose and the linear increase of peak-to-peak height with the square root of microwave power in the absence of saturation indicate that gamma radiation induces, in NS, radical species having similar saturation characteristics but different formation and decay rates. The broad singlet line is possibly due to carboxyl-free radical ($R-CHCH_3-COO^{\bullet}$) of different orientational and environmental features produced by preferential rupture of O–Na in the crystalline (ionic bonds) NS matrix. In fact NS crystallizes in monoclinic system with $P2_1$ symmetry and contains two molecules per unit cell (Ravikumar et al., 1985). Carboxyl radicals giving rise to broad singlet resonance line have been also observed in gamma-irradiated carboxylic acid (Iwasaki, 1972) and ceftazidime (Miyazaki et al., 1994). Although a guess concerning the origin of the radicals I and II, which give rise to NS ESR signal, can be made, it is not the case for AP due to the higher number of component in the excipient part. However, one can conclude from the dose–response curve given in Fig. 4 that the radical formation energies in the excipient part are lower than those for radicals I and II.

3.4. Radical decays

The rates of radical decay depend on the nature of the solid matrix (Tilquin, 1985). Annealing is a constant process with local diffusion of radicals and molecules in some softening of defects or irregularities. At room temperature, the radical decay is very slow and many radical–molecule reactions observed in the liquid state are not responsible. The results indicate that peak-to-peak height decay behavior obtained for NS can be explained by a homogeneous kinetic, such as second-order kinetic with a constant value of the rate. Therefore, numerical simulations of the results were performed using bi-exponential model (Table 3). Clearly, the model parameter's fit is acceptable, within the error ($< 3\%$).

Typical decay behavior obtained in the present study above room temperature (Table 2) shows that in NS a two-step radical decay is clearly present, suggesting the presence of two radical species with different decay constant (Onori et al., 1996). However, at room temperature no decay was detected for NS. This indicates that the radical concentrations are likely to remain stable for a long time (Fig. 6a). The latter feature provides to NS and to pharmaceuticals containing NS as active ingredient such as AP a desired feature to estimate absorbed radiation doses, even a long time after the irradiation process.

The biphasic character of AP room temperature decay arises from the features of the contributing radicals. Although one of the contributing radicals decays very fast, the others decay slower. In 2 days, the contribution of fast-decaying radical becomes negligible and peak-to-peak height is governed by two radicals from NS part and one from excipient part of AP. Fast decay observed above 338 K originates from the decay of the radicals I and I′ which have decay activation energies of 40.7 and 31.8 (kJ/mol), respectively.

3.5. Radiosensitivity of AP and applicability of ESR technique to monitor radiosterilization of AP

Radiation sensitivity of a substance or mixture is expressed by g-value, which is the number of radicals produced by the absorbed radiation dose per 100 eV. A higher concentration of radicals, generated at the same absorbed dose of radiation, indicates a higher sensitivity of the substance toward gamma radiation. However, the efficiency of microcrystalline matrices for trapping paramagnetic species also has to be considered. It is known that the influence of some substituents on radical population is stronger than others. One of the

most significant groups that increase radical concentration is carboxyl-containing substituent, which is the case for NS and AP.

The number of free radicals in Fig. 4 was estimated by comparison of the second integrals obtained from irradiated sample spectra recorded and the linear part of dose–response curve and the DPPH standard. To get an integrated relative area, all spectra were corrected for baseline using a linear function and doubly integrated. The number of free radicals estimated by this procedure was $(8 \pm 2)\ 10^{15}$ spin/g/kGy. From this a g-value of 0.13 was found. This value is 1 for alanine (Ikeya, 1993). The ESR signal recorded for AP is specific for radiation treatment because no ESR signal was detected in unirradiated samples. Relatively big half-times of three contributing radicals of high weights provide a long time stability to the ESR signal at room temperature (Fig. 6). Therefore, ESR can be used safely to get both qualitative information (i.e. whether or not AP has been irradiated) and quantitative results (i.e. the dose it received) up to the recommended maximum radiosterilization dose which has been established by many regulatory authorities (EN 552, 1994; ISO 11137, 1995), because the contributing radicals are quite stable, the relative signal is clearly distinguishable from that of reference sample and the signal is relatively constant to estimate initial dose.

4. Conclusion

Gamma irradiation of NS and AP produces free radicals which are detectable by ESR and appear to be relatively stable at room temperature but highly unstable above room temperature. The two radicals designed I and II of different formation and decay characteristics contribute to the ESR singlet observed for irradiated NS, and two more radicals I′ and II′′ arising from the excipient part are involved in the formation of multi-line ESR spectrum of irradiated AP. Therefore, ESR measurements can be used for the detection and discrimination of unirradiated NS and AP from irradiated ones. The increase in the peak-to-peak height versus dose was simulated using exponential and linear regression analysis. The shape of decay curve over a storage period of 0–60 days at room temperature indicates that the free radicals could be detected even after a storage period of several months in both NS and AP. However, radicals created in the excipient part (I′, II′′) which contribute efficiently to the intensity of the singlet resonance line arising from active component degradation of AP, i.e. from NS, create an increase of approximately twofold in the peak-to-peak height of the $g = 2.0057$ singlet. This causes an improvement in the detection limit in favor of AP.

The results given above indicate that the two basic requirements of specificity and stability are met in irradiated NS and AP. Therefore, ESR technique can be used in monitoring the radiosterilization of NS containing drugs, if samples are stored in proper conditions. A reliable judgement about a possible irradiation can be done if the test is performed within a suitable storage time.

References

Basly, J.P., Longy, I., Bernard, M., 1998. Radiosterilization dosimetry by electron spin resonance spectroscopy: cefotetan. Anal. Chim. Acta 359, 107–113.

Bittner, B., Mader, K., Kroll, C., Borchert, H.H., Kissel, T., 1999. Tetracycline–HCI-loaded poly(D,L-lactide–co–glycolide) microspheres prepared by spray drying technique: influence of γ-irradiation on radical formation and polymer degradation. J. Control. Release 59, 23–32.

Boess, C., Bögl, K.W., 1996. Influence of radiation treatment on pharmaceuticals—a review: alkoloids, morphine derivatives and antibiotics. Drug Dev. Ind. Pharm. 22, 495–529.

Bögl, K.W., 1989. Identification of irradiated foods—methods, development and concepts. Appl. Radiat. Isot. 40, 1203–1210.

Bozdağ, S., Çaliş, S., Kas, H.S., Ercan, M.T., Peksoy, I., Hincal, A.A., 2001. In vitro evaluation and intra-articular administration of biodegradable microspheres containing naproxen sodium. J. Microencapsul. 18, 443–456.

Çaliş, S., Bozdağ, S., Kaş, H.S., Tunçay, M., Hincal, A.A., 2002. Influence of irradiation sterilization on poly(lactide–co–glycolide) microspheres containing anti-inflammatory drugs. IL Farmaco. 57, 55–62.

Christensen, E.A., Holm, N.W., Juul, F.A., 1967. Radiosterilization of medical devices and supplies. In: Radiosterilization of Medical Products (STI/PUB/157). IAEA, Vienna, pp. 265–286.

Desrosiers, M.F., Simic, M.G., 1988. Postirradiation dosimetry of meat by electron spin resonance spectroscopy of bones. J. Agric. Food Chem. 36, 601–603.

Dood, N.J.F., Swallow, A.J., Lea, F.J., 1985. Use of ESR to identify irradiated food. Radiat. Phys. Chem. 26, 451–453.

Duroux, J.L., Basly, J.P., Penicaut, B., Bernard, M., 1996. ESR spectroscopy applied to the study of drugs radiosterilization: case of three nitroimidazoles. Appl. Radiat. Isot. 47, 1565–1568.

Dusaucy, A.C., Tilquin, B., 1991. Selectivity in dehydrodimerization of amides: final product analysis from radiolysis in the liquid phase. Radiat. Phys. Chem. 37, 217–220.

EN 552, 1994. Sterilization of medical devices—validation and routine control of sterilization by irradiation, CEN, European Committee for Standardization, Brussels, Belgium.

Gaughran, E.R.L., Goudie, A.J., 1977. Sterilization by Ionizing Radiation: Sterilization of Medical Products by Ionizing Radiation, vol. II. Multiscience Publishers Ltd., Montreal, Quebec.

Gibella, M., Crucq, A.-S., Tilquin, B., Stocker, P., Lesgards, G., Raffi, J.J., 2000. Electron spin resonance studies of some irradiated pharmaceuticals. Radiat. Phys. Chem. 58, 69–76.

Ikeya, M., 1993. New Applications of Electron Spin Resonance, Dating, Dosimetry and Microscopy. World Scientific, Singapore, p. 399.

ISO 11137, 1995. Sterilization of health care products—requirement for validation and routine control—radiation sterilization, International Organization for Standardization, Geneva, Switzerland.

Iwasaki, M., 1972. MTP Phys. Chem. Ser., Int. Rev. Sci. 4, 317–346.

Jacobs, G.P., 1991. Radiation in the sterilization of pharmaceuticals. In: Sterile Pharmaceutical Manufacturing, vol. I, 1st ed.. Interpharm. Press, Buffalo Grove, IL, pp. 57–78.

Jacobs, G.P., 1995. A review of the effects of gamma-radiation on pharmaceutical materials. J. Biomed. Appl. 10, 59–96.

Korkmaz, M., Polat, M., 2000. Free radical kinetics of irradiated durum wheat. Radiat. Phys. Chem. 58, 169–179.

Korkmaz, M., Polat, M., 2001. Radical kinetics and characterization of the free radicals in gamma irradiated red pepper. Radiat. Phys. Chem. 62, 411–421.

Miyazaki, T., Kaneko, T., Yoshimura, T., Crucq, A.S., Tilquin, B., 1994. Electron spin resonance study of radiosterilization of antibiotics: ceftazidime. J. Pharm. Sci. 83, 68–71.

Onori, S., Pantaloni, M., Fattibene, P., Ciranni, E.S., Valvo, L., Santucci, M., 1996. ESR identification of irradiated antibiotics: cephalosporins. Appl. Radiat. Isot. 47, 1569–1572.

Polat, M., Korkmaz, M., Dulkan, B., Korkmaz, Ö., 1997. Detection of irradiated chicken and dosimetric properties of drumsticks bones. Radiat. Phys. Chem. 49, 363–369.

Pourahmad, R., Pakravan, R., 1997. Radiosterilization of disposable medical devices. Radiat. Phys. Chem. 49, 285–286.

Raffi, J.J., 1992. Electron spin resonance intercomparison studies on irradiated foodstuffs. Commission of the European Communities, Luxemburg, Belgium, EUR 13630 EN, 1992.

Ravikumar, K., Rajan, S.S., Pattabhi, V., 1985. Structure of naproxen, $C_{14}H_{14}O_3$. Acta Crystallogr. C 41, 280–282.

Reid, B.D., 1995. Gamma processing technology: an alternative technology for terminal sterilization of parenterals. PDA J. Pharm. Sci. Technol. 49, 83–89.

Safrany, A., 1997. Radiation processing: synthesis and modification of biomaterials for medical use. Nucl. Inst. Methods Phys. Res. B 131, 376–381.

Schuler, R.H., 1994. Three decades of spectroscopic studies of radiation produced intermediates. Radiat. Phys. Chem. 43, 417–423.

Tilquin, B., 1985. Composant radicalaire des transformations radio-initieés dans les alcanes à 77 K, Thèse d'agrégation, UCL, Ciaco-la-Neuve, Belgique.

Volland, C., Wolff, M., Kissel, T., 1994. The influence of terminal gamma-sterilization on captopril containing poly(D,L-lactide–co–glycolide) microspheres. J. Control. Release 31, 293–305.